Reduction of Dispersion-Induced Distortion in SCM Transmission Systems by Using Predistortion-Linearized MQW–EA Modulators

Takanori Iwai, *Member, IEEE*, Kenji Sato, and Ko-ichi Suto, *Member, IEEE*

***Abstract*—The application of low-chirp MQW (multiquantum well)–EA (electro-absorption) modulators to subcarrier multiplexing (SCM) optical transmission systems is studied. The authors show that a third-order predistortion circuit is feasible for compensating the nonlinearity of this type of modulator. The degree of frequency chirping per optical intensity modulation depth of the modulator is theoretically determined to be about 1.4 MHz. A 42-channel AM–SCM signal transmitter with the predistortion circuit realizes both composite second-order distortion (CSO) and composite triple beat distortion (CTB) values under −57 dBc after 200-km-long transmission. The authors confirm dispersion-induced distortion of the MQW–EA modulator is as small as that of the $LiNbO_3$ modulator. Carrier-to-noise ratios (CNR's) of 45.2 dB for channel 1 and 43.8 dB for channel 42 were measured after 100 km transmission. It is found that the deterioration of a CNR is caused by the cascaded erbium doped fiber amplifiers (EDFA's), Rayleigh backscattered power and the optical phase noise. Theoretical CNR's show that the output power of the modulator should be higher to improve CNR.**

***Index Terms*—Electro-absorption modulators, optical communications, subcarrier multiplexing.**

I. Introduction

RECENT advances in optical amplification technique using erbium doped fiber amplifiers (EDFA's) have stimulated the investigation of subcarrier mutliplexing (SCM) video distribution systems that use fiber star feeders [1]–[5]. These systems will realize economical all-fiber video distribution (AFVD) that allows many subscribers to share large parts of both the transmitter and the transmission line sections. The 1.55 μm EDFA's would be used in the transmitter sections even though the transmission line sections would retain the conventional 1.3 μm zero-dispersion single-mode fibers already deployed. Under this high wavelength-dispersion condition, SCM transmission systems experience serious performance deterioration due to the dispersion-induced nonlinear distortion caused by the combined action of fiber dispersion and the frequency chirp of the optical transmitter [6], [7].

There are two candidates for reducing dispersion-induced distortion: dispersion compensation fibers (DCF's) [8]–[10] and a low-chirp optical transmitters. The former, which places appropriate lengths of opposite-sign DCF's in the transmitter section, is too inflexible in terms of accepting transmission length differences. The application of DCF's is not suitable for AFVD subscriber networks because the transmission length differs for each subscriber.

The latter candidate, low chirp optical transmitters that reduce dispersion-induced distortion, is beneficial in the sense that dispersion management becomes unnecessary. Low-chirp lasers [11]–[14] based on multiquantum-well (MQW) structures are one of the candidates. The linewidth enhancement factor (α-parameter) has been reduced to as small as 1.0 [12]. However, the nonlinear distortion generated by the nonlinearity of this type of DFB laser should be reduced to implement practical analog video signal transmission systems [15], [16].

Another low-chirp optical source is the external modulator which generally offers low-chirp and high-speed modulation characteristics [17], [18]. $LiNbO_3$ Mach–Zehnder external modulators [19], [20] have been mainly investigated for SCM transmission systems [21]–[23]. It has already been reported that an 80-channel AM–SCM transmission system employing this type of modulator can successfully achieve 30 km-long transmission with low noise and low distortion [23]. Practical transmission systems that employ this type of modulator need a control electric circuit to offset the fluctuation of the L–V (light power versus voltage) curve in the direction of voltage, i.e., the dc drift effect [24]–[26].

Multiquantum-well electro-absorption (MQW–EA) type optical modulators [27]–[34] have been actively investigated because of the high-efficiency electro-absorption effect, the quantum-confined Stark effect (QCSE). Their high-speed, low-chirp, and low-power consumption characteristics are suitable for application to optical communication systems. MQW–EA external modulators are dc drift free and can be monolithically integrated with DFB lasers [35]–[37]. Furthermore, this type of modulator offers lower power consumption than $LiNbO_3$ Mach–Zehnder type modulators.

Table I compares the performances of a $LiNbO_3$ Mach–Zehnder modulator and an MQW–EA modulator. The α-parameter of a $LiNbO_3$ modulator can be controlled by the bias voltages applied to its two electrodes. The small chirp condition, instead of the chirp-free condition, is used to reduce dispersion penalty. The α-parameter of MQW–EA modulators is less than one and the value is small compared

Manuscript received January 18, 1996; revised September 4, 1996.

T. Iwai is with NTT Multimedia Business Department, Chiyoda-ku, Tokyo 100, Japan.

K. Sato is with NTT Opto-electronics Laboratories, Atsugi-shi, Kanagawa-ken, 243-01, Japan.

K. Suto is with NTT Multimedia Networks Laboratories, Yokosuka-shi, Kanagawa-ken 238-03, Japan.

Publisher Item Identifier S 0733-8724(97)01376-5.

TABLE I
PERFORMANCE COMPARISON OF $LiNbO_3$ MODULATOR AND MQW–EA MODULATOR

modulator	α-parameter	insertion loss	bandwidth	bias voltage	DC drift	LD integration	nonlinearity
$LiNbO_3$ modulator	[18] small & controllable	[19] 4 dB	[20] 75 GHz	[19] 3.6 V	needs control circuit	difficult	third-order (sinusoidal)
MQW-EA modulator	[17],[28] < 1	[33] 8 dB	[33] 50 GHz	0.63 V	null	suitable	unknown

with the value of conventional DFB lasers, 2–7, [17]. The insertion loss of the MQW–EA modulator is at present larger than that of the $LiNbO_3$ modulator. Both modulators have great potential for ultrahigh-speed operation. Low power consumption and dc drift free MQW–EA modulators can be fabricated as integrated optical sources that do not need a dc drift control circuit.

This paper investigates the feasibility of the MQW–EA modulator in SCM transmission systems [38]–[41]. We propose a feasible predistortion linearization method that offsets the nonlinearity of the modulator. Transmission experiments show the validity of the predistortion method. The degree of the modulator's frequency chirping is theoretically estimated.

We report the nonlinear distortion and CNR characteristics of SCM transmission systems that employ the linearized MQW–EA modulator, 1.3 μm zero-dispersion single-mode fiber, and EDFA's. The results of 42-channel AM–SCM signal transmission are presented in the paper. The measured results for distortion are compared with the theoretical results allowing the degree of frequency chirping of the modulator to be determined. The origins of carrier-to-noise ratio (CNR) deterioration and the methods for increasing the CNR are discussed on the basis of the theoretical results considering relative intensity noise (RIN) deterioration due to Rayleigh backscattered power and cascaded EDFA's.

The paper is organized as follows. Section II analyzes the distortion caused by the nonlinearity of MQW–EA modulators. An electrical predistortion technique that minimizes the nonlinear distortion is proposed and its feasibility is examined using multichannel SCM signals. Section III derives the degree of frequency chirping in MQW–EA modulators. Section IV details an AM–VSB signal transmission experiment. Calculated results based on the theories provided in Section III and theoretical CNR deterioration are included in the discussions. Finally, Section V concludes this paper.

II. PREDISTORTION LINEARIZATION TECHNIQUE

It has been already found that the L–V curve of a $LiNbO_3$ Mach–Zehnder modulator is a sinusoidal curve and third-order nonlinearity is dominant at its inflection point. A predistortion linearization circuit that compensates third-order nonlinear distortion is generally used in conjunction with the modulator. In the case of the MQW–EA modulator, the cause of nonlinearity has not been fully clarified.

We examined the modulator consisting of strained-InGaAsP MQW's grown on an n-type substrate by low pressure MOVPE [29]. The modulator was mounted on a microwave strip line and terminated with a 50 Ω resistor. Fig. 1 shows the measured optical power output by a typical modulator. A bias voltage, V_b, and electrical and optical modulation depths of the modulator, m_0 and m, are illustrated in the figure. It is found that modulator's nonlinearity distorts the output signal. Insertion loss of the modulator at the applied voltage of 0 V is about 10 dB.

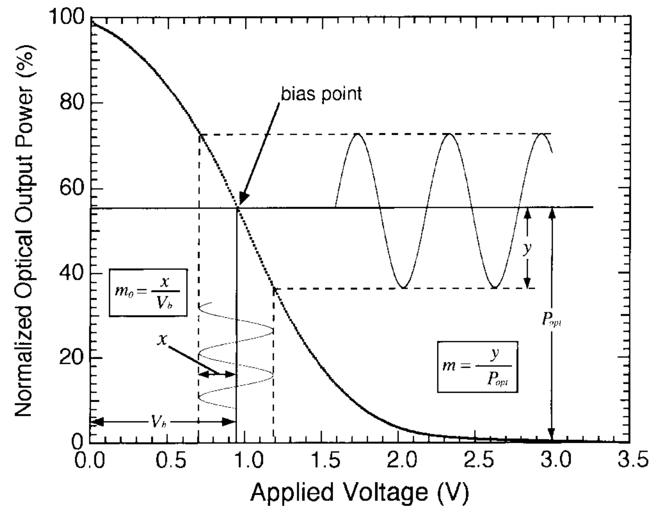

Fig. 1. Normalized (100% at 0 V) optical output power from a typical MQW–EA modulator as a function of the applied voltage. m_0: electrical modulation depth, m: optical modulation depth.

The power intensity, $P_{\rm opt}$, of the modulator output from the EA modulator can be approximated as a function of the applied voltage V as [28], [30]

$$P_{\rm opt} = P_0 \exp[-(V/V_0)^a] \tag{1}$$

where P_0 and V_0 are the output at the voltage of 0 V and the voltage when the output is P_0/e, respectively. Parameter a is 2–4 for MQW type modulators [30]. In the case of single-tone modulation, V in (1) is expressed as

$$V = V_b[1 + m_0 \cos(\omega t)] \tag{2}$$

where ω is the modulation angular frequency.

The second-order and third-order intermodulation distortion, IMD2 and IMD3, caused by two RF signals can be theoretically calculated using the expansion coefficients of (1)

$$\text{IMD2} = \left[\frac{a(V_b/V_0)^{a-1} - (a-1)(V_b/V_0)^{-1}}{2V_0}(m_0 V_b)\right]^2 \tag{3}$$

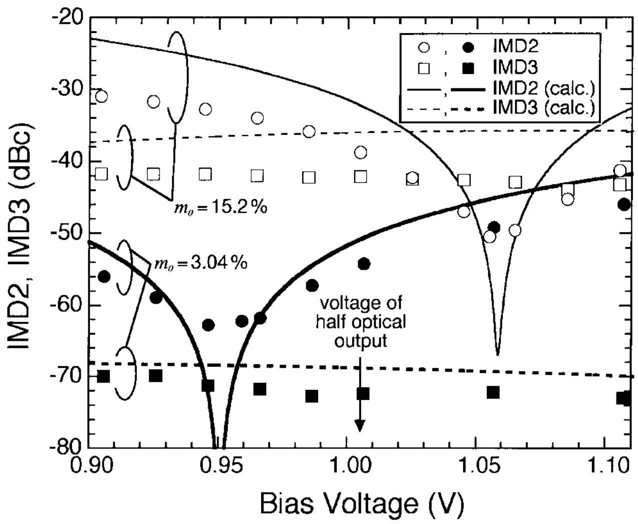

Fig. 2. The IMD2 and IMD3 as functions of the bias voltage. The modulation frequencies of the two RF signals are 211.25 MHz and 217.25 MHz, respectively.

and (4) shown at the bottom of the page. The derivations of (3) and (4) are shown in Appendix A.

Fig. 2 shows experimental and calculated results for IMD2 and IMD3 in the case $m_0 = 15.2$ and $m_0 = 3.04\%$ as functions of the bias voltage. The IMD2 calculation considers the contribution of fourth-order nonlinearity. The modulation depths were determined at the bias voltage of 0.95 V and the electrical power was kept constant regardless of the bias voltage. This means the value of $m_0 V_b$ in (3) and (4) is constant regardless of the change of V_b. In the calculation the values of V_0 and $m_0 V_b$ were assumed to have the same values as recorded in the measurement: $V_0 = 1.19$ V and $m_0 V_b = 0.95 m_0$ V. The value of a is chosen to fit the measured results: $a = 2.4$ for $m_0 = 3.04\%$ and $a = 3.2$ for $m_0 = 15.2\%$. Calculated results well reflect the experimental ones and the feasibility of (1) as an approximate equation of the L–V characteristics is shown. Calculated results in Fig. 2 show that the nonlinear characteristic of the modulator strongly depends on a. It is found that the asymmetry around the bias point yields different optimum bias voltages giving minimum IMD2 for different modulation depths.

One reason for the discrepancy of the minimum values between theoretical and measured results is considered to be the deviation of the real L–V characteristic around the bias point from (1). This was verified by the fact that in Fig. 2 the discrepancy for the case of $m_0 = 15.2\%$ is more serious than for the case of $m_0 = 3.04\%$. Another reason is the effect of higher order nonlinearity of the modulator. The IMD2 calculation that does not consider fourth-order nonlinearity enlarges the discrepancy by 4.5 dB and 40 dB for the case of $m_0 = 3.04$ and $m_0 = 15.2\%$, respectively. Taking much higher order terms into account will reduce the discrepancy further.

From (3), the bias voltage ($V_{\min}$) which gives the minimum IMD2 is given by (see Appendix A)

$$V_{\min} = \left(\frac{a-1}{a}\right)^{\frac{1}{a}} V_0. \tag{5}$$

Under the bias voltage condition of (5), for $a = 2$–4

$$P_{\text{opt}} = e^{-\frac{a-1}{a}} P_0 \approx 0.61 P_0 - 0.47 P_0. \tag{6}$$

This means $V_{\min}$ is around the value that gives half the optical output recorded when the bias voltage is 0 V (see Fig. 1).

Fig. 2 shows that the second-order distortion can be minimized by adjusting the bias voltage so that the optical output power is around half the value recorded when the applied voltage is 0 V. A low-distortion optical transmitter can be constructed by selecting the appropriate bias voltage and using the predistortion circuit that compensates third-order distortion.

The proposed predistortion linearization method has two parts.

1) Setting the bias voltage to achieve around one half of the optical output yielded when the bias voltage is 0 V so that the second-order distortion is minimized for the modulation depth of the target system.
2) Under the above bias voltage condition, applying the predistortion circuit to compensate third-order distortion.

We examined the feasibility of our predistortion technique through the transmission of multichannel SCM carriers. Fig. 3 shows CTB improvement under the optimum bias voltage condition for 42 channel AM–VSB carrier transmission as a function of AM band frequency. The inset illustrates the predistortion circuit examined here. We constructed the circuit using a push-pull operated diode circuit [23]. The predistortion circuit yields a 9 to 12 dB improvement in CTB which was held to under −60 dBc over the entire AM band. The measured back-to-back CSO results were less than −60 dBc regardless of the predistortion circuit used.

The electric predistortion linearization circuit shown in Fig. 3 was designed to compensate the third-order distortion, CTB, caused by the nonlinearity of the modulator [21]–[23]. The original SCM signal is split and one part is directly input to the modulator through a delay line. The other part is used to generate CTB. The CTB signal is input to the modulator so as to cancel the distortion generated by the modulator and this minimizes the CTB of the transmitter. From Fig. 3 it is shown that our predistortion technique is adaptable to multichannel SCM signal transmission.

III. Frequency Chirping of MQW–EA Modulators

The degree of dispersion-induced distortion depends on the degree of frequency chirping of the optical transmitter. We theoretically estimate the frequency chirping of an MQW–EA

$$\text{IMD3} = \left[\frac{-a^2(V_b/V_0)^{2a-2} + 3a(a-1)(V_b/V_0)^{a-2} - (a-1)(a-2)(V_b/V_0)^{-2}}{8V_0^2}(m_0 V_b)^2\right]^2. \tag{4}$$

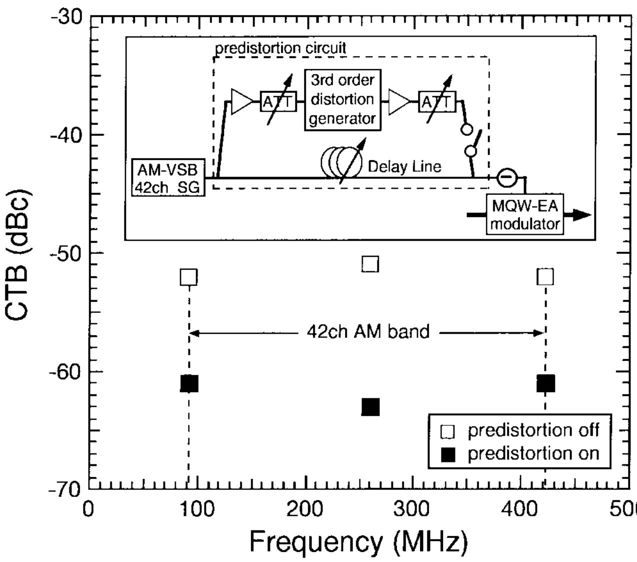

Fig. 3. The CTB improvement for a 42-channel AM–VSB signal as a function of AM band frequency. The inset shows the predistortion circuit examined here. ATT: electrical attenuator.

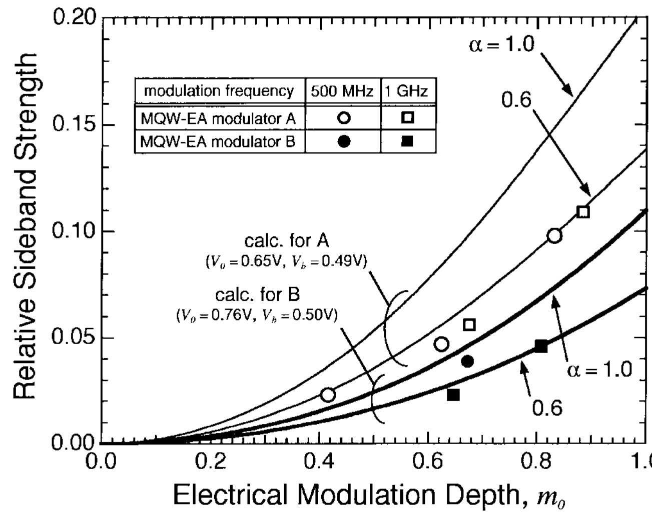

Fig. 4. Relative sideband strength as a function of the modulation depth as per [28] and [30]. In the calculations, the value of a is assumed to be three and V_b and V_0 take their experimental values.

modulator. Assuming that the α-parameter is independent of m, the phase ϕ of the light output by the EA modulator is related to the α-parameter as [17]

$$\frac{d\phi}{dt} = \frac{\alpha}{2P_{\text{opt}}}\frac{dP_{\text{opt}}}{dt}. \tag{7}$$

We estimated the frequency chirping of the modulator from FM efficiency. FM efficiency β is defined as frequency chirping per intensity modulation depth of each carrier. Usually β is expressed as frequency chirping per injection current. In this paper we evaluate the frequency chirping of a current-driven DFB laser and voltage-driven external modulators. Therefore, we express FM efficiency as the frequency chirping per modulation depth. β (Hz/%) is defined as

$$\beta = \frac{1}{2\pi \cdot 100m}\frac{d\phi}{dt}\bigg|_{\text{0-peak}}. \tag{8}$$

Note β is usually expressed as 0-peak value. We use (1) as P_{opt} in (7). Substituting (7), (1) and (2) into (8) yields

$$\beta = \frac{\alpha a \omega}{400\pi}\left(\frac{m_0}{m}\right)\left(\frac{V_b}{V_0}\right)^a [1 + m_0\cos(\omega t)]^{a-1}\sin(\omega t)\bigg|_{\text{0-peak}}. \tag{9}$$

In the case of composite modulation, the total electrical and total optical modulation depths [42], [43] are applied to (9) instead of m_0 and m, respectively. If $m_0 \ll 1$ and $m_0 \approx m$, (9) reduces to

$$\beta \approx \frac{\alpha a \omega}{400\pi}\left(\frac{V_b}{V_0}\right)^a \sin(\omega t)\bigg|_{0-\text{peak}} = \frac{\alpha a \omega}{400\pi}\left(\frac{V_b}{V_0}\right)^a. \tag{10}$$

We estimated the α-parameter of the modulator by measuring its relative sideband strength [28], [30], [31]. Fig. 4 shows the experimental results and calculations [28], [30] for two different modulators as a function of m_0. From this figure the value of the α-parameter is estimated to be about 0.6. Using $\alpha = 0.6$ we estimated the frequency chirping of the MQW–EA modulator according to (9). Total electrical modulation depth (M_0) and total optical modulation depth (M) are given as follows:

$$M_0 = \sqrt{Nm_0^2/2} \tag{11}$$

$$M = \sqrt{Nm^2/2} \tag{12}$$

where N is channel number and $N = 42$ in our experiment. The values of V_0, V_b, m_0 and m were the same as recorded in the transmission experiment described in Section IV: $V_0 = 0.85$ V, $V_b = 0.63$ V and $m_0 = m = 0.04$. For $a = 2$–4, the value of β is calculated to be 1.5–1.6 MHz/% at the modulation frequency of 421.25 MHz ($\omega = 2\pi \cdot 421.25$ (Mrad/s)) which is the carrier frequency of the forty-second channel. It is found that the value of β for the modulator is quite small compared to usual DFB lasers which have values of several dozens of MHz/%.

Dispersion-induced distortion, CSO, at frequency f_d is expressed using β as

$$\text{CSO} \approx (200\pi)^2 Cm^2 (f_d DL\beta\lambda^2/c)^2. \tag{13}$$

$C, D,$ and L are the composite number, fiber dispersion, and fiber length, respectively. λ and c indicate the wavelength and the speed of light in a vacuum, respectively. The derivation of (13) is shown in Appendix B.

IV. A 42-Channel AM–VSB Signal Transmission Experiment

A. Experimental Set-Up

We conducted an AM–SCM transmission experiment to examine the feasibility of our predistortion technique and the validity of our theoretical estimation of the frequency

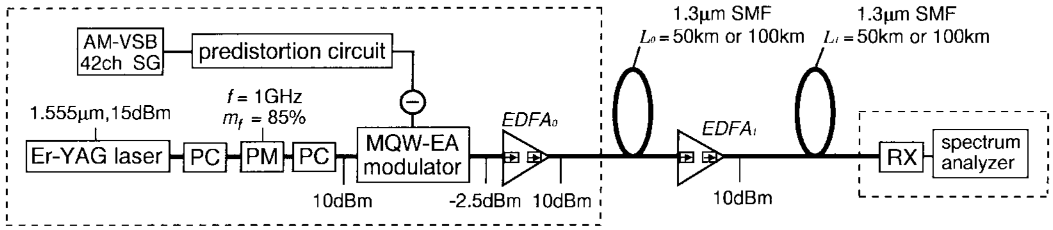

Fig. 5. Experimental setup for 42 channel AM–SCM signal transmission. SG: signal generator, PC: polarization controller, and PM: phase modulator.

chirping of the modulator. Furthermore CNR dependence on transmission length was evaluated both experimentally and theoretically. Fig. 5 shows the experimental setup for the 42-channel AM–VSB transmission experiment. An Er-YAG laser was used as the optical source and its wavelength and linewidth were 1.555 μm and 20 kHz, respectively.

In order to increase the threshold optical power of stimulated Brillouin scattering (SBS) [44], the optical power was distributed over a number of optical subcarrier by single-tone phase-modulation. The modulation depth and frequency of the $LiNbO_3$ waveguide phase modulator were 0.85 and 1 GHz, respectively. As a result the threshold optical power increased up to 10 dBm for 100 km-long transmission, which is higher by as much as 3 dB than the power of no phase modulation condition.

The optical modulation depth of the AM–VSB carriers ranging from 91.25 MHz to 421.25 MHz was adjusted to 4% per channel. The carrier allocation was based on the frequency arrangement of Japanese CATV systems. The measured RIN's of the light input to the transmitter EDFA and the output light were -156 and -147 dB/Hz, respectively. We examined AM–VSB signal transmission using two cascaded EDFA's. The power of two EDFA's output to 1.3 μm zero-dispersion SMF (nondispersion-shifted fiber, NDSF) was 10 dBm. A launch power of 10 dBm allows us to neglect the CSO degradation by self-phase modulation [45]. Different transmission distances were used in the distortion measurements (200 km) and CNR measurements (100 km). To accurately estimate the value of the modulator's frequency chirping, a 200 km-long transmission experiment was conducted.

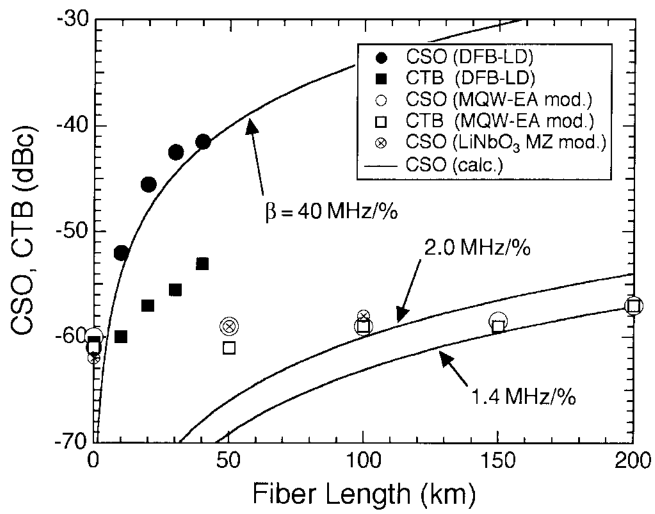

Fig. 6. The CSO and CTB dependence on transmission length for MQW–EA modulator, $LiNbO_3$ modulator and directly-modulated DFB laser. The carrier frequency is 421.25 MHz (the forty-second channel).

TABLE II
CALCULATION PARAMETERS FOR (13)

Parameters	Value
Fiber Dispersion, D (ps/nm/km)	16.5
Speed of Light, c (m/s)	3×10^8
Composite Number, C	12.5
Laser Wavelength, λ (nm)	1555.0
Optical Modulation Depth per Carrier, m	0.04
Distortion Frequency, f_d (MHz)	422.5

B. Results and Discussions

Measured CSO and CTB are shown in Fig. 6 as a function of transmission length. It is found from the figure that the MQW–EA modulator transmitter has a range of 200 km if both CSO and CTB ≤ -57 dBc. Directly modulating a conventional DFB laser yields a much shorter transmission range. Measured CSO with a $LiNbO_3$ modulator is also plotted in the figure. It is found that the $LiNbO_3$ modulator's frequency chirping is of the same degree as that of the MQW–EA modulator.

Solid lines in Fig. 6 are the CSO degradation calculated by (13). Calculation parameters are shown in Table II. The calculated lines demonstrate that the MQW–EA modulator's frequency chirping is as small as 1.4 MHz/%. This value is in good agreement with the theoretical value of 1.5–1.6 MHz which confirms that the frequency chirping of the modulator is as small as 1.4 MHz/%.

The measured CNR dependence on transmission length is shown in Fig. 7(a) and (b). CNR's of 45.2 dB for channel 1 [Fig. 7(a)] and 43.8 dB for channel 42 [Fig. 7(b)] were measured after 100 km transmission. CNR deteriorates due to the RIN degradation caused by the noise figures (NF's) of the cascaded EDFA's [3], [5], Rayleigh backscattered power [5], [46], [47] and the optical phase noise [48]. Rayleigh backscatter is generated by the combined action of the laser light and the fiber refractive index inhomogeneities along the transmission path. Backscattered light causes the signal-double backscatter noise that happens when the backscattered light is scattered again by the fiber refractive index inhomogeneities toward the receiver [5]. The optical phase noise of an optical transmitter deteriorates the RIN of the transmission system by

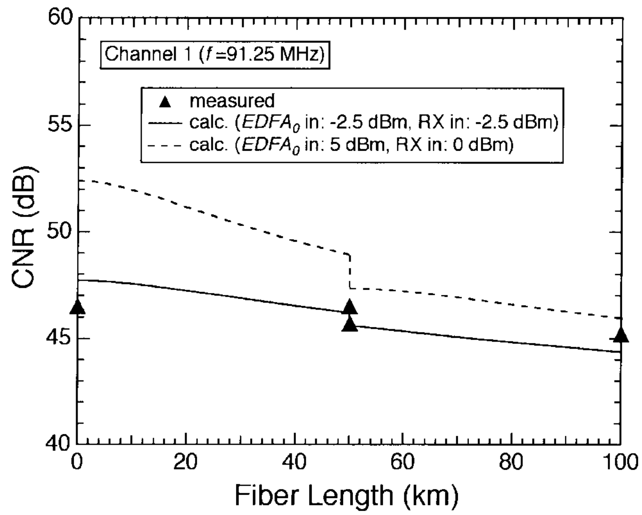

(a)

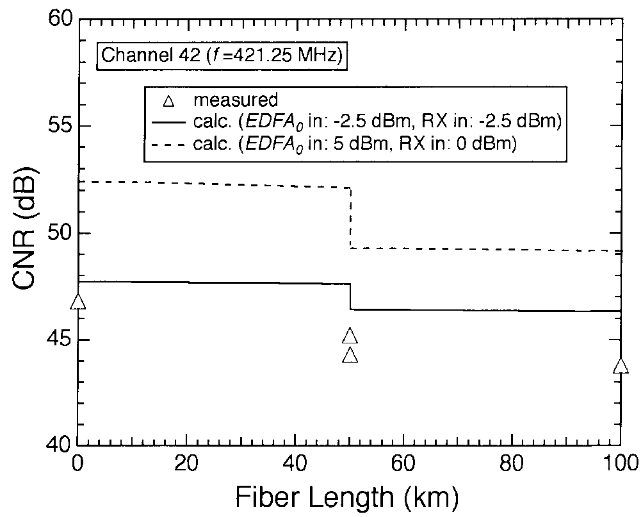

(b)

Fig. 7. A CNR dependence on transmission length. (a) The measured frequency is 91.25 MHz (the first channel). (b) The measured frequency is 421.25 MHz (the forty-second channel).

the FM–AM noise conversion in the dispersive single-mode fiber.

If we assume RIN_0 as the RIN of the modulator output light and RIN_1 as the RIN caused by the influence of the noise figures (NF's) of cascaded EDFA's and Rayleigh backscattered noise, CNR is expressed as follows:

$$\mathrm{CNR} = \frac{\frac{1}{2}(mrP_{\mathrm{rec}})^2}{[I_{\mathrm{th}}^2 + 2erP_{\mathrm{rec}} + (\mathrm{RIN}_0 + \mathrm{RIN}_1)(rP_{\mathrm{rec}})^2]B}. \quad (14)$$

Here $r, P_{\mathrm{rec}}, I_{\mathrm{th}}$ indicate O/E conversion efficiency, received optical power, and thermal noise current of the receiver amplifier, respectively. B denotes bandwidth. We consider a transmission system with a transmitter amplifier (EDFA_0) and n_r repeater amplifiers (EDFA_1, EDFA_2, $\cdots$, EDFA_{n_r}) under random polarization. If it is assumed that L and L_n are the transmission length and the interval between the nth repeater amplifier and the $(n+1)$th repeater amplifier or the receiver,

TABLE III
CALCULATION PARAMETERS FOR (14) AND (15)

Parameters	Value
O/E conversion efficiency, r	0.86
Thermal Noise Current, I_{th} ($pA/\mathrm{Hz}^{1/2}$)	10
Bandwidth, B (MHz)	4.2
Energy of A Photon, $h\nu$ (J)	1.27×10^{-19}
Product of Fiber Capture Factor (S) and Rayleigh Backscatter Coefficient (α_s), $S\alpha_s$ (Neper^2/km^2)	0.043
Fiber Loss, α' (Neper/km)	3.5×10^{-5}
Frequency of Interest, f (MHz)	91.25 or 421.25
Fiber Length, L_0, L_1 (km)	50
Transmitter EDFA ($EDFA_0$) Noise Figure , NF_0 (dB)	6.2
Repeater EDFA ($EDFA_1$) Noise Figure , NF_1 (dB)	6.2
$EDFA_0$ Input Optical Power , P_{in_0} (dBm)	-2.5
$EDFA_1$ Input Optical Power , P_{in_1} (dBm)	0
Laser Linewidth $\Delta\nu$, (MHz)	37
Modulation Depth per Carrier, m	0.04
Laser RIN, RIN_0 (dB/Hz)	-156
Received Optical Power, P_{rec} (dBm)	-2.5 or 0

respectively, after the nth amplifier $(0 \leq n \leq n_r)$ RIN_1 at frequency f is approximately given by [3], [5], [47]

$$\begin{aligned}\mathrm{RIN}_1 \approx \sum_{k=0}^{n} \frac{2hv \cdot NF_k}{P_{\mathrm{in}_k}} + \frac{2}{\pi}\frac{\Delta v}{\Delta v^2 + f^2}\left(\frac{S\alpha_s}{2\alpha'}\right)^2 \\ \times \left[2\alpha' L - (n+1) + \sum_{k=0}^{n-1} e^{-2\alpha' L_k} \right. \\ \left. + e^{-2\alpha'\left(L - \sum_{k=0}^{n-1} L_k\right)}\right]. \quad (15)\end{aligned}$$

Note if $n = 0$, the terms, $\sum_{k=0}^{n-1} e^{-2\alpha' L_k}$ and $\sum_{k=0}^{n-1} L_k$ equal zero. Δv and hv denote the unmodulated linewidth of the laser light and the energy of the light, respectively. P_{in_k} and NF_k are the input power to the kth EDFA and the noise figure of the kth EDFA, respectively. S, α_s, and α' are the fraction of scattering captured by the fiber, the proportion of the signal scattered per unit length, and fiber loss per unit length, respectively [5], [46], [47]. In (15), we ignore the reflection backscatter effect caused by the multiple reflection of backscattered light in the fiber.

The solid lines in Fig. 7(a) and (b) show calculated CNR deterioration using (14) and (15) assuming the same calculation parameters with measurement which are shown in Table III. The discrepancy between calculated and measured values in Fig. 7(b) is considered to be caused by the optical phase noise. The influence of the optical phase noise is serious at high channel number [48], and our results reflect the fact. The influence of the optical phase noise should be reduced by narrowing the linewidth of the MQW–EA modulator input light which was broadened to up to 37 MHz (the linewidth of the center subcarrier) by the chirping of the phase modulator in our experiments.

The dashed lines in Fig. 7(a) and (b) were calculated assuming that the optical power input to the transmitter EDFA is 5 dBm by means of (14) and (15); this means that the effect of phase noise is not considered. The figures show that the transmitter EDFA input power of 5 dBm achieves a CNR of 49 dB entire AM band after 50 km transmission, which is quite a feasible transmission distance for subscriber networks. Considering video quality, in 1990 the Electronic and Industries Association of Japan (EIAJ) evaluated the relation of CNR value to mean opinion score (MOS) [49] as scaled by the International Radio Consultative Committee (CCIR) [50]. The EIAJ measured CNR value of 49 dB corresponds to a MOS of 4.5 which is graded as the mean of “Excellent” (MOS of five) and “Good” (MOS of four). The EDFA input power of 5 dBm can be achieved by reducing the insertion loss of the modulator, or using a high power optical source or an integrated DFB laser/modulator transmitter. The insertion loss of 8 dB has been reported [33] and further improvement is possible by shortening the waveguide length or increasing the coupling efficiency by using optical fibers [51]. The output of the integrated light source can be increased by improving the efficiency of the MQW structure of the DFB laser section [52]–[54].

V. Conclusion

The feasibility of the MQW–EA modulator for SCM transmission was examined. It was shown that the nonlinearity of the modulator is well canceled by the proposed third-order predistortion linearization technique. From a 42-channel AM–VSB signal transmission experiment, the frequency chirping of the modulator was determined to be as small as 1.4 MHz/% and the feasibility of the modulator in reducing dispersion-induced distortion was clarified. We verified the degree of dispersion-induced distortion of the MQW–EA modulator is as small as that of the $LiNbO_3$ modulator by means of the AM–SCM signal transmission experiment. The CNR degradation was caused by the RIN degradation due to Rayleigh backscattered power, cascaded EDFA’s and the optical phase noise. Increasing the input optical power to the transmitter EDFA, that is the optical power output from the MQW–EA modulator, is essential in increasing the CNR.

Appendix A
Derivation of (3) to (6)

The relation of a modulator input signal $e_{\rm in}$ and the output signal $e_{\rm out}$ is

$$e_{\rm out} = K_1 e_{\rm in} + K_2 e_{\rm in}^2 + K_3 e_{\rm in}^3 + \cdots \tag{A1}$$

where K_1, K_2, and K_3 are the linear (first-order) coefficient, the second-order distortion coefficient, and the third-order distortion coefficient, respectively. In the case that two the RF signals have modulation angular frequencies of ω_1 and ω_2 and amplitudes of A_1 and A_2, respectively, $e_{\rm in}$ is given by

$$e_{\rm in} = A_1 \cos(\omega_1 t) + A_2 \cos(\omega_2 t). \tag{A2}$$

The substitution of (A2) into (A1) yields second-order intermodulation distortion coefficient (IMC2) and third-order intermodulation coefficient (IMC3) as follows:

$$\mathrm{IMC2} = K_2 A_1 A_2 \cos[(\omega_1 \pm \omega_2)t] \tag{A3}$$

$$\begin{aligned}\mathrm{IMC3} &= (3/4) K_3 A_1^2 A_2 \cos[(2\omega_1 \pm \omega_2)t],\\ &\quad (3/4) K_3 A_2^2 A_1 \cos[(2\omega_2 \pm \omega_1)t].\end{aligned} \tag{A4}$$

Here, we ignore the contribution of more than third-order terms. We assume $A_1 = A_2 = A$. IMD2 and IMD3 are given by

$$\mathrm{IMD2} = \left(\frac{\mathrm{IMC2}|_{0-\mathrm{peak}}}{K_1 A}\right)^2 \tag{A5}$$

$$\mathrm{IMD3} = \left(\frac{\mathrm{IMC3}|_{0-\mathrm{peak}}}{K_1 A}\right)^2. \tag{A6}$$

Equation (1) can be developed around the bias voltage V_b as shown in (A7) at the bottom of the page. The value of A in our experiment is $m_0 V_b$ and the value is constant regardless of the change of V_b (see Section II). From (A7) K_1, K_2, and K_3 are determined as

$$K_1 = -\frac{a(V_b/V_0)^{a-1}}{V_0} P_0 \exp[-(V_b/V_0)^a] \tag{A8}$$

$$\begin{aligned}K_2 &= \frac{a^2(V_b/V_0)^{2a-2} - a(a-1)(V_b/V_0)^{a-2}}{2V_0^2} P_0\\ &\quad \times \exp[-(V_b/V_0)^a]\end{aligned} \tag{A9}$$

and (A10) shown at the bottom of the page. IMD2 and IMD3 are then expressed using (A5) and (A6) as follows.:

$$\begin{aligned}\mathrm{IMD2}\\ &= \left\{\frac{[a^2(V_b/V_0)^{2a-2} - a(a-1)(V_b/V_0)^{a-2}]/2V_0^2}{-a(V_b/V_0)^{a-1}/V_0}(m_0 V_b)\right\}^2\\ &= \left[\frac{a(V_b/V_0)^{a-1} - (a-1)(V_b/V_0)^{-1}}{2V_0}(m_0 V_b)\right]^2\end{aligned} \tag{A11}$$

and (A12) shown at the top of the next page.

$$\begin{aligned}P_{\rm opt} = P_0 \exp[-(V_b/V_0)^a] \times \Bigg[1 &- \frac{(V_b/V_0)^{a-1}}{V_0}(V - V_b) + \frac{a^2(V_b/V_0)^{2a-2} - a(a-1)(V_b/V_0)^{a-2}}{2V_0^2}(V - V_b)^2\\ &+ \frac{-a^3(V_b/V_0)^{3a-3} + 3a^2(a-1)(V_b/V_0)^{2a-3} - a(a-1)(a-2)(V_b/V_0)^{a-3}}{6V_0^3}\\ &\times (V - V_b)^3 + \cdots\Bigg].\end{aligned} \tag{A7}$$

$$K_3 = \frac{-a^3(V_b/V_0)^{3a-3} + 3a^2(a-1)(V_b/V_0)^{2a-3} - a(a-1)(a-2)(V_b/V_0)^{a-3}}{6V_0^3} \times P_0 \exp[-(V_b/V_0)^a]. \tag{A10}$$

$$\begin{aligned}\mathrm{IMD3} &= \left\{\frac{3}{4}\frac{[-a^3(V_b/V_0)^{3a-3}+3a^2(a-1)(V_b/V_0)^{2a-3}-a(a-1)(a-2)(V_b/V_0)^{a-3}]/6V_0^3}{-a(V_b/V_0)^{a-1}/V_0}(m_0V_b)^2\right\}^2 \\ &= \left[\frac{-a^2(V_b/V_0)^{2a-2}+3a(a-1)(V_b/V_0)^{a-2}-(a-1)(a-2)(V_b/V_0)^{-2}}{8V_0^2}(m_0V_b)^2\right]^2. \qquad \text{(A12)}\end{aligned}$$

In (A11), equating $\mathrm{IMD2} = 0$ gives the bias voltage $(V_{\min})$ of the inflection point.

$$V_{\mathrm{IMD2=0}} = \left(\frac{a-1}{a}\right)^{\frac{1}{a}} V_0. \qquad \text{(A13)}$$

Substituting (A13) to (1) yields the optical output at the inflection point.

$$P_{\mathrm{opt}} = e^{-\frac{a-1}{a}} P_0 \qquad \text{(A14)}$$

Appendix B
Derivation of (13)

B.

CSO degradation due to the combined action of frequency chirping and fiber dispersion is given by [7]

$$\mathrm{CSO} = Cm^2\bar{p}^2(dp/dI)^{-2}\frac{A^2+(2\pi f_d)^2E^2}{G^2+(2\pi f_c)^2H^2} \qquad \text{(A15)}$$

where $\bar{p}, dp/dI$ are averaged output power of the modulator, and optical slope efficiency, respectively. f_c and f_d indicate the carrier and distortion frequency, respectively. The coefficients A, E, G, and H are given as

$$A = \alpha_a \frac{1}{2}\frac{d^2p}{dI^2} \qquad \text{(A16)}$$

$$E = \alpha_a DL\frac{dv}{dI}\frac{dp}{dI}\frac{\lambda^2}{c} \qquad \text{(A17)}$$

$$G = \alpha_a \frac{dp}{dI} \qquad \text{(A18)}$$

$$H = \bar{p}DL\frac{dv}{dI}\frac{\lambda^2}{c}. \qquad \text{(A19)}$$

$\alpha_a, dv/dI$, and d^2p/dI^2 are system attenuation coefficient, frequency chirping, and optical superlinearity of the modulator, respectively. In our experiment, $A \approx 0$ because the modulator is operated near its inflection point to minimize second-order nonlinearity (see Section II). Furthermore, the value of α_a is about 0.2 even in the case of 200 km-long transmission because of cascaded EDFA's (see Section IV).

If we assume linear optical output near the bias point, dv/dI and dp/dI can be written using β, V_b and the impedance (Z) of the device including the drive circuit as

$$\frac{dv}{dI} = \frac{100\beta}{(V_b/Z)} \qquad \text{(A20)}$$

$$\frac{dp}{dI} = \frac{\bar{p}}{(V_b/Z)}. \qquad \text{(A21)}$$

Using (A20) and (A21) and assuming $A = 0$, we can rewrite (A15) as

$$\begin{aligned}\mathrm{CSO} &= \frac{Cm^2\alpha_a^2(f_d/f_c)^2}{1+\alpha_a^2(200\pi f_c DL\beta\lambda^2/c)^{-2}} \\ &\approx (200\pi)^2Cm^2(f_dDL\beta\lambda^2/c)^2. \qquad \text{(A22)}\end{aligned}$$

Acknowledgment

The authors would like to express their sincere gratitude to T. Kanada, K. Sano, N. Shibata, K. Kikushima, and H. Yoshinaga for several useful discussions.

References

[1] R. Olshansky and E. Eichen, "Microwave-multiplexed wideband lightwave systems using optical amplifiers for subscriber distribution," *Electron. Lett.*, vol. 24, pp. 922–923, July 1988.

[2] W. I. Way, M. M. Choy, A. Yi-Yan, M. Andrejco, M. Saifi, and C. Lin, "Multi-channel AM-VSB television signal transmission using an erbium-doped optical fiber power amplifier," in *Proc. IOOC'89*, Kobe, Japan, July 1989, paper 20PDA-10.

[3] E. Yoneda, K. Suto, K. Kikushima, and H. Yoshinaga, "All-fiber video distribution (AFVD) systems using SCM and EDFA techniques," *J. Lightwave Technol.*, vol. 11, pp. 128–137, Jan. 1993.

[4] D. J. M. Sabido IX, M. Tabara, T. K. Fong, and L. G. Kazovsky, "Experimental investigation of the impact of EDFA's on coherent AM analog optical links," in *Proc. OFC'94*, San Jose, CA, Feb. 1994, paper ThS4.

[5] D. A. Atlas, R. Pidgeon, and F. Little, "Rayleigh backscatter effects on 1550-nm CATV distribution systems employing optical amplifiers," *J. Lightwave Technol.*, vol. 13, pp. 933–946, May 1995.

[6] M. Shigematsu, K. Nakazato, T. Okita, Y. Tagami, and K. Nawata, "Field test of multichannel AM-VSB transmission using an erbium doped optical fiber amplifier at 1.55 μm wavelength range in the CATV network," in *Proc. Topical Meeting on Optical Amplifiers and Their Applications*, Montrey, CA, Aug. 1990, paper WB3.

[7] E. E. Bergmann, C. Y. Kuo, and S. Y. Huang, "Dispersion-induced second-order distortion at 1.5 μm," *IEEE Photon. Technol. Lett.*, vol. 3, pp. 59–61, Jan. 1991.

[8] K. Kikushima, "Using equalizers to offset the deterioration in SCM video transmission due to fiber dispersion and EDFA gain tilt," *J. Lightwave Technol.*, vol. 10, pp. 1443–1449, Oct. 1992.

[9] A. Bjarklev, T. Rasmussen, O. Lumholt, K. Rottwitt, and M. Helmer, "Optimal design of single-cladded dispersion-compensating optical fibers," *Opt. Lett.*, vol. 19, pp. 457–459, Apr. 1994.

[10] A. J. Antos and D. K. Smith, "Design and characterization of dispersion compensating fiber based on the LP_{01} mode," *J. Lightwave Technol.*, vol. 12, pp. 1739–1745, Oct. 1994.

[11] Y. Miyake and M. Asada, "Spectral characteristics of linewidth enhancement factor α of multidimensional quantum wells," *Japan. J. Appl. Phys.*, vol. 28, pp. 1280–1281, July 1989.

[12] F. Kano, T. Yamanaka, N. Yamamoto, Y. Yoshikuni, H. Mawatari, Y. Tohmori, M. Yamamoto, and K. Yokoyama, "Reduction of linewidth enhancement factor in InGaAsP-InP modulation-doped strained multiple-quantum-well lasers," *IEEE J. Quantum Electron.*, vol. 29, pp. 1553–1559, June 1992.

[13] H. Mawatari, F. Kano, N. Yamamoto, Y. Kondo, Y. Tohmotri, and Y. Yoshikuni, "Spectral linewidth and linewidth enhancement factor in 1.5 μm modulation-doped strained MQW lasers," in *Proc. SSDM'93*, Chiba, Japan, Aug. 1993, paper D-7-1.

[14] A. Schönfelder, S. Weisser, J. D. Ralston, and J. Rosenzweig, "Differential gain, refractive index, and linewidth enhancement factor in

high-speed GaAs-based MQW lasers: Influence of strain and p-doping," *IEEE Photon. Technol. Lett.*, vol. 6, pp. 891–893, Aug. 1994.

[15] T. Okuda, H. Yamada, T. Torikai, and T. Uji, "Novel partially corrugated waveguide laser diode with low modulation distortion characteristics for subcarrier multiplexing," *Electron. Lett.*, vol. 26, pp. 862–863, May 1994.

[16] N. Otsuka, M. Kito, M. Ishio, J. Ohya, Y. Kudo, and Y. Matsui, "1.5 μm strained-layer MQW-DFB lasers with low chirp and low distortion characteristics," in *Proc. IOOC'95*, Hong Kong, June 1995, paper FB2-5.

[17] F. Koyama and K. Iga, "Frequency chirping in external modulators," *J. Lightwave Technol.*, vol. 6, pp. 87–93, Jan. 1988.

[18] K. Hagimoto, T. Kataoka, Y. Miyamoto, K. Sato, and K. Noguchi, "Ultra-high-speed modulation technology for IM/DD systems," in *Proc. ECOC'93*, Montreux, Switzerland, Sept. 1993, paper MoC1.4.

[19] K. Noguchi, O. Mitomi, K. Kawano, and M. Yanagibashi, "Highly efficient 40-GHz bandwidth Ti:$LiNbO_3$ optical modulator employing ridge structure," *IEEE Photon. Technol. Lett.*, vol. 5, pp. 52–54, Jan. 1993.

[20] K. Noguchi, O. Mitomi, H. Miyazawa, and S. Seki, "A broadband Ti: $LiNbO_3$ optical modulator with a ridge structure," *J. Lightwave Technol.*, vol. 13, pp. 1164–1168, June 1995.

[21] R. B. Childs and V. A. O'Byrne, "Multichannel AM video transmission using a high-power Nd:YAG laser and linearized external modulator," *IEEE J. Select. Areas Commun.*, vol. 8, pp. 1369–1376, Sept. 1990.

[22] T. Lang and J. Bissinger, "CATV distribution in an FITL network," in *Proc. 3rd IEEE Workshop on Local Opt. Networks*, Tokyo, Japan, Sept. 1991, paper G2.

[23] M. Nazarathy, J. Berger, A. J. Ley, I. M. Levi, and Y. Kagan, "Progress in externally modulated AM CATV transmission systems," *J. Lightwave Technol.*, vol. 11, pp. 82–105, Jan. 1993.

[24] R. V. Schmidt, P. S. Cross, and A. M. Glass, "Optically induced crosstalk in $LiNbO_3$ waveguide switches," *J. Appl. Phys.*, vol. 51, pp. 90–93, Jan. 1980.

[25] R. A. Becker, "Circuit effect in $LiNbO_3$ channel-waveguide modulators," *Opt. Lett.*, vol. 10, pp. 417–419, Aug. 1985.

[26] H. Jumonji and T. Nozawa, "Instabilities and their characterization in Mach-Zehnder Ti:$LiNbO_3$ optical modulators," *IEICE Trans. C-I*, vol. J75-C-I, pp. 17–26, Jan. 1992 (in Japanese).

[27] I. Kotaka, K. Wakita, K. Kawano, M. Asai, and M. Naganuma, "High-speed and low-driving-voltage InGaAs/InAlAs multiquantum well optical modulators," *Electron. Lett.*, vol. 27, pp. 2162–2163, Nov. 1991.

[28] O. Mitomi, S. Nojima, I. Kotaka, K. Wakita, K. Kawano, and M. Naganuma, "Chirping characteristic and frequency response of MQW optical intensity modulator," *J. Lightwave Technol.*, vol. 10, pp. 71–77, Jan. 1992.

[29] K. Sato, K. Wakita, and M. Yamamoto, "Strained InGaAsP multi-quantum wells for optical electroabsorption waveguide modulators," *Electron. Lett.*, vol. 26, pp. 609–610, Mar. 1992.

[30] O. Mitomi, K. Wakita, and I. Kotaka, "Chirping characteristic of electroabsorption-type optical-intensity modulator," *IEEE Photon. Technol. Lett.*, vol. 6, pp. 205–207, Feb. 1994.

[31] T. H. Wood, L. M. Ostar, and M. Suzuki, "The effect of modulator nonlinearity on measurements of chirp in electroabsorption modulators," *J. Lightwave Technol.*, vol. 12, pp. 1152–1158, July 1994.

[32] F. Devaux, S. Chelles, J. C. Harmand, N. Bouadma, F. Huet, M. Carre, and M. Foucher, "Polarization independent InGaAs/InAlAs strained MQW electroabsorption modulator with 42 GHz bandwidth," in *Proc. IOOC'95*, Hong Kong, June 1995, paper FB3-2.

[33] T. Ido, S. Tanaka, M. Suzuki, and H. Inoue, "An ultra-high-speed (50 GHz) MQW electro-absorption modulator with waveguides for 40 Gbit/s optical modulation," in *Proc. IOOC'95*, Hong Kong, June 1995, post-deadline paper PD1-1.

[34] K. Wakita, I. Kotaka, T. Amano, and H. Sugiura, "1.3 μm waveguided electroabsorption modulators with strain-compensated InAsP/InGaP MQW structures," *Electron. Lett.*, vol. 31, pp. 1339–1341, Aug. 1995.

[35] K. Sato, I. Kotaka, K. Wakita, Y. Kondo, and M. Yamamoto, "Strained-InGaAsP MQW electroabsorption modulator integrated DFB laser," *Electron. Lett.*, vol. 29, pp. 1087–1088, June 1993.

[36] K. Wakita, K. Sato, I. Kotaka, M. Yamamoto, and T. Kataoka, "20 Gbit/s, 1.55 μm strained-InGaAsP MQW modulator integrated DFB laser module," *Electron. Lett.*, vol. 30, pp. 302–303, Feb. 1994.

[37] T. Kataoka, Y. Miyamoto, K. Hagimoto, K. Sato, I. Kotaka, and K. Wakita, "20 Gbit/s transmission experiments using an integrated MQW modulator/DFB laser module," *Electron. Lett.*, vol. 30, pp. 872–873, May 1994.

[38] G. C. Willson, T. H. Wood, S. B. Krasulick, J. E. Johnson, T. Tanbun-Ek, and P. A. Morton, "Linearization of an integrated electroabsorption modulator/DFB laser using electronic predistortion," in *Proc. CLEO'95*, Baltimore, MD, May 1995, post-deadline paper CDP-12.

[39] T. Iwai, H. Yoshinaga, K. Suto, and K. Sato, "AM-SCM video transmission experiment employing MQW-EA external modulator and predistortion linearization technique," in *Proc. IOOC'95*, Hong Kong, June 1995, paper FC2-3.

[40] T. Iwai and K. Sato, "Dispersion-induced distortion in AM-SCM transmission systems employing linearized MQW-EA modulator," *Electron. Lett.*, vol. 31, pp. 1272–1273, July 1995.

[41] T. Iwai, K. Sato, and K. Suto, "Signal distortion and noise in AM-SCM transmission systems employing the feedforward linearized MQW-EA external modulator," *J. Lightwave Technol.*, vol. 13, pp. 1606–1612, Aug. 1995.

[42] F. V. C. Mendis and B. T. Tan, "Overmodulation in subcarrier multiplexed video FM broad-band optical networks," *J. Select. Areas Commun.*, vol. 8, pp. 1285–1289, Sept. 1990.

[43] T. E. Darcie, G. E. Bodeep, and A. A. M. Saleh, "Fiber-reflection-induced impairments in lightwave AM-VSB CATV systems," *J. Lightwave Technol.*, vol. 9, pp. 991–995, Aug. 1991.

[44] H. Yoshinaga, "Influence of stimulated Brillouin scattering on nonlinear distortion in SCM video transmission," *Electron. Lett.*, vol. 29, pp. 1707–1708, Sept. 1993.

[45] F. W. Willems, W. Muys, and J. C. van der Paats, "Experimental verification of self-phase-modulation-induced nonlinear distortion in externally modulated AM-VSB lightwave systems," in *Proc. OFC'96*, San Jose, CA, Feb. 1996, paper ThR4.

[46] A. F. Judy, "Intensity noise from fiber Rayleigh backscatter and mechanical splices," in *Proc. ECOC'89*, Gothenburg, Sweden, Sept. 1989, paper TuP-11.

[47] A. F. Judy, "Generation of interference intensity noise from fiber Rayleigh backscatter and discrete reflections," in *Proc. OFC'91*, San Jose, CA, Feb. 1991, paper WL4.

[48] C. Y. Kuo, D. Piehler, C. Gall, J. Kleefeld, A. Nilsson, and L. Middleton, "High-performance optically amplified 1550-nm lightwave AM-VSB CATV transport system," in *Proc. OFC'96*, San Jose, CA, Feb. 1996, paper WN2.

[49] T. Izumi, Ed., *Cable Television Technology*. Tokyo, Japan: Corona, 1994, p. 193 (in Japanese).

[50] CCIR Recommendation AA/II: Method for subjective assessment of the quality of television pictures CCIR conclusions of the Interim meeting of study group (Genova) Part I, pp. 165–168, 1982.

[51] Y. Tohmori, Y. Suzaki, H. Fukano, M. Okamoto, Y. Sakai, O. Mitomi, S. Matsumoto, M. Yamamoto, M. Fukuda, M. Wada, Y. Itaya, and T. Sugie, "Spot-size convered 1.3 μm laser with butt-jointed selectively grown vertically tapered waveguide," *Electron. Lett.*, vol. 31, pp. 1069–1070, June 1995.

[52] P. J. A. Thijis, L. F. Tiemeijer, P. I. Kuindersma, J. J. M. Bisma, and T. V. Dongen, "High-performance 1.5 μm wavelength InGaAs-InGaAsP strained quantum well lasers and amplifiers," *IEEE J. Quantum Electron.*, vol. QE-27, pp. 1426–1439, June 1991.

[53] H. Lu, C. Blaauw, B. Benyon, G. P. Li, and T. Makino, "High-power and high-speed performance of 1.3-μm strained MQW gain-coupled DFB lasers," *IEEE J. Select. Topics Quantum Electon.*, vol. 1, pp. 375–381, June 1995.

[54] D. I. Babic, K. Streubel, R. P. Mirin, N. M. Margalit, J. E. Bowers, E. L. Hu, D. E. Mars, L. Yang, and K. Carey, "Room-temperature continuous-wave operation of 1.54-μm vertical-cavity lasers," in *Proc. IOOC'95*, Hong Kong, June 1995, post-deadline paper PD1-5.

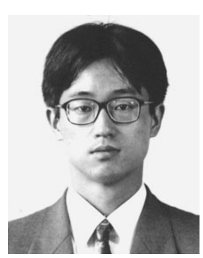

Takanori Iwai (A'94-M'95) was born in Gifu Prefecture, Japan, in October 1966. He received the B.E. and M.E. degrees from Kyoto University, Kyoto, Japan, in 1990 and in 1992, respectively.

In 1992, he joined the NTT Electrical Communication Laboratories and had worked in the NTT Optical Network Systems Laboratories, Kanagawa-ken, Japan, for four years. Since 1996, he has been engaged in business development on the application of high-speed access networks in the NTT Multimedia Business Department, Tokyo, Japan. His research interest there included optical fiber loop subscriber transmission systems.

Mr. Iwai is a member of the Physical Society of Japan and the Institute of Electronics, Information and Communication Engineers (IEICE) of Japan.

Kenji Sato received the B.S. degree in 1978, the M.S. degree in 1980, and the Ph.D. degree in 1992 from the Nagoya University, Nagoya, Japan.

In 1980, he joined the NTT Electrical Communications Laboratories. He is now a Senior Research Engineer with NTT Opto-electronics Laboratories, Kanagawa, Japan. His current research interests include long-wavelength lasers, modulators, and optical short-pulse sources.

Dr. Sato is a member of the Physical Society of Japan, the Japan Society of Applied Physics, and the Institute of Electronics, Information and Communication Engineers (IEICE) of Japan.

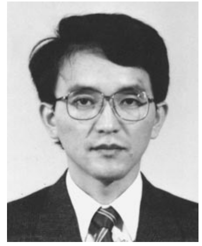

Ko-ichi Suto (M'95) was born in Niigata Prefecture, Japan, in 1955. He received the B.S. degree from Iwate University in 1977.

Since joining the NTT Laboratories in 1977, he has been active in developmental research on optical fiber subscriber trunk transmission systems. Since 1983, he has been engaged in developmental research on optical fiber subscriber loop transmission systems. He is now a Senior Research Engineer, Supervisor of NTT Multimedia Networks laboratories, Kanagawa-ken, Japan.

Mr. Suto is a member of the Institute of Electronics, Information and Communication Engineers (IEICE) of Japan.